Ca^{2+} and Ionic Strength Dependencies of S1-ADP Binding to Actin-Tropomyosin-Troponin: Regulatory Implications

Boris Gafurov,† Yi-Der Chen,* and Joseph M. Chalovich†

*Laboratory of Biological Modeling, National Institute of Diabetes and Digestive and Kidney Diseases, National Institutes of Health, Bethesda, Maryland 20892-5621; and †Department of Biochemistry and Molecular Biology, Brody School of Medicine at East Carolina University, Greenville, North Carolina 27858-4354

ABSTRACT Skeletal and cardiac muscle contraction are inhibited by the actin-associated complex of tropomyosin-troponin. Binding of Ca^{2+} to troponin or binding of ATP-free myosin to actin reverses this inhibition. Ca^{2+} and ATP-free myosin stabilize different tropomyosin-actin structural arrangements. The position of tropomyosin on actin affects the binding of ATP-free myosin to actin but does not greatly affect myosin-ATP binding. Ca^{2+} and ATP-free myosin alter both the affinity of ATP-free myosin for actin and the kinetics of that binding. A parallel pathway model of regulation simulated the effects of Ca^{2+} and ATP-free myosin binding on both equilibrium binding of myosin-nucleotide complexes to actin and the general features of ATPase activity. That model was recently shown to simulate the kinetics of myosin-S1 binding but the analysis was limited to a single condition because of the limited data available. We have now measured equilibrium binding and binding kinetics of myosin-S1-ADP to actin at a series of ionic strengths and free Ca^{2+} concentrations. The parallel pathway model of regulation is consistent with those data. In that model the interaction between adjacent regulatory complexes fully saturated with Ca^{2+} was destabilized and the inactive state of actin was stabilized at high ionic strength. These changes explain the previously observed change in binding kinetics with increasing ionic strength.

INTRODUCTION

Striated muscle contraction is regulated by a protein complex bound to actin. The complex of tropomyosin, troponin T, troponin I, and troponin C inhibits ATPase activity under resting, low Ca^{2+}, conditions. An increase in Ca^{2+} results in an 80-fold increase in ATPase activity (Chalovich and Eisenberg, 1982). A further eightfold increase in ATPase rate occurs with the addition of high concentrations of NEM-S1 (Williams et al., 1988), a modified myosin subfragment that binds tightly to actin even in the presence of ATP. In solution, the binding of NEM-S1 or other ''activating'' forms of myosin can elevate the ATPase activity to about the same level regardless of the presence of Ca^{2+} (Williams et al., 1988). Furthermore, the affinity of S1-ADP and rigor S1 for actin is enhanced by both Ca^{2+} and binding of S1 to actin (Greene and Eisenberg, 1980). The rate of S1 and S1-ADP binding are also increased by both Ca^{2+} and the occupancy of actin with bound S1 (Trybus and Taylor, 1980; Geeves and Halsall, 1987). In contrast, the affinity of S1 to actin during the hydrolysis of ATP is not greatly affected by Ca^{2+} or by S1 binding (Chalovich et al., 1981; Chalovich, 1992). These observations have been interpreted in terms of different models of regulation. Identifying reasonable models of regulation is important because of the role of defects in muscle regulatory proteins in cardiac failure (Thierfelder et al., 1994) and other disorders.

Tropomyosin-troponin undergoes a rapid structural change upon activation (Kress et al., 1986) but the number of discrete functional states and the role of each of these states is uncertain. This change was postulated to be a movement of tropomyosin into the actin groove (Parry and Squire, 1973; Haselgrove and Huxley, 1973). Recent observations suggest that there may be three positions of tropomyosin on actin (Vibert et al., 1997; Poole et al., 1995) although it is uncertain if there are three discrete functional states (Perry, 2003). The possibility has been raised that troponin contributes to the observed movement (Hai et al., 2002; Chalovich, 2002). In the relaxed state tropomyosin overlaps the putative site of S1-ADP binding but not the site of S1-ATP binding (Craig and Lehman, 2001). Thus there is good agreement between structural and biochemical data.

We favor the view that regulation of striated muscle contraction involves transitions among two or more parallel pathways of ATP hydrolysis. Ca^{2+} and ATP-free myosin binding are activators that stabilize states of the actin filament that have enhanced activities toward actin-activated ATP hydrolysis (Chalovich et al., 1981; Hill et al., 1981; Chalovich and Eisenberg, 1982). The parallel pathway model is based upon the idea that the cooperative activation of ATPase activity (Eisenberg and Weihing, 1970; Murray et al., 1982) results from multiple states of actin with distributions that are determined by Ca^{2+} and S1-ADP or rigor S1 binding (Greene and Eisenberg, 1980, 1988). Fig. 1 *A* shows this model having parallel pathways of ATP

Submitted March 25, 2004, and accepted for publication June 22, 2004.

Address reprint requests to Joseph M. Chalovich, Dept. of Biochemistry and Molecular Biology, Brody School of Medicine at East Carolina University, 600 Moye Blvd., Greenville, North Carolina 27834. Tel.: 252-744-2973; Fax: 252-744-3383; E-mail: chalovichj@mail.ecu.edu.

Abbreviations used: NEM, *N*-ethyl maleimide; Ap5A, P^1,P^5-di(adenosine-5′) pentaphosphate; S1, myosin subfragment 1; regulated actin, actin-tropomyosin-troponin.

0006-3495/04/09/1825/11 $2.00

doi: 10.1529/biophysj.104.043364

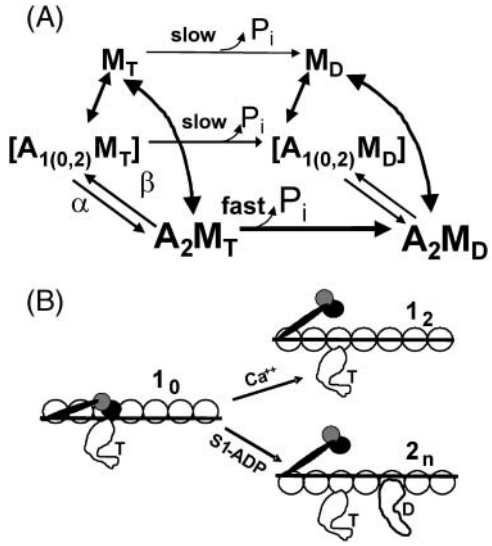

FIGURE 1 Parallel pathways of ATP hydrolysis in the Hill model of regulation. In the scheme M is myosin with bound ATP (subscript T) or ADP (subscript D), A is actin-tropomyosin in either the inactive (A_1) or active (A_2) state. (*A*) Actin-tropomyosin-troponin can exist in two or three states that are in equilibrium. ATP hydrolysis is slow if myosin-ATP is bound to regulated actin in state 1 but rapid if bound to actin in state 2. Ca^{2+} and ATP-free myosin increase the population of state 2. Because two states were sufficient to explain regulation of ATPase activity the properties of state 1 were assumed to be the same with either 0 or two bound Ca^{2+} (hence the notation $A_{1(0,2)}$). Three functional states of regulated actin can be accommodated by assuming that the properties of state 1 with 2 bound Ca^{2+} lie between those of states 1_0 and 2. (*B*) Possible assignment of states in the Hill model to the three putative structural states. Ca^{2+} binding to state 1_0 stabilizes state 1_2 by weakening the interaction between troponin and actin and allowing tropomyosin to move to an intermediate position. S1-ADP binding to states 1_0 or 1_2 stabilizes regulated actin in state 2 where tropomyosin is in its most extreme position. The properties of state 2 are independent of the number of bound Ca^{2+} ($n = 0$, 1, or 2).

hydrolysis for free S1, and for S1 bound to actin in state 1 (inactive) and state 2 (active). A model based on two functional actin states of actin was sufficient to simulate equilibrium binding of S1 to actin (Hill et al., 1980) and actin-activated ATPase activity (Hill et al., 1981).

The inclusion of a third functional actin state was thought to be necessary to explain the effect of Ca^{2+} on the rate of binding of S1-ADP or S1 to regulated actin. That third state, the blocked state, was proposed to be unable to bind to S1 (McKillop and Geeves, 1993). We recently used Monte Carlo methods to analyze binding kinetics by the parallel pathway Hill model (Chen et al., 2001). The two-state Hill model predicted the same binding kinetics as a model that included the blocked state. However, that former analysis was too restricted to adequately test either model's ability to simulate real data under a variety of experimental conditions. A rigorous test of models of regulation requires an extensive data set that includes equilibrium binding, binding kinetics, and ATPase activities under the same conditions.

We have now compiled a data set for the binding of S1-ADP to regulated actin for testing models of regulation. Equilibrium binding was measured at six free Ca^{2+} concentrations at each of six ionic strength conditions. Binding kinetics were measured for many of these same conditions. Both the Hill model and a model containing a blocked state were fitted to the equilibrium binding curves to obtain the parameters describing equilibrium binding as a function of ionic strength and free Ca^{2+}. Inclusion of a blocked state was unnecessary for simulating equilibrium binding and binding kinetics. Thus two states are sufficient for explaining regulatory function. The model is also consistent with a third functional state should that be required. The results are consistent with the idea that tropomyosin-troponin is an allosteric switch (Hill et al., 1981; Resetar et al., 2002; Heeley et al., 2002).

MATERIALS AND METHODS

Protein preparation

Actin (Spudich and Watt, 1971; Eisenberg and Kielley, 1972), myosin (Kielley and Harrington, 1960), and troponin and tropomyosin (Eisenberg and Kielley, 1974) were isolated from rabbit back muscle. Myosin-S1 was made by digestion of myosin with chymotrypsin (Weeds and Taylor, 1975). Protein concentrations were determined by light absorbance at 280 nm, corrected for scattering at 340 nm, using the following extinction coefficients ($\varepsilon^{0.1\%}$) for 280 nm: actin, 1.15; myosin-S1, 0.75; tropomyosin, 0.33; troponin, 0.37.

Actin was labeled with *N*-(1-pyrenyl)iodoacetamide (Kouyama and Mihashi, 1981) and stored as a 40-μM stock in 4 mM imidazole (pH 7.0), 1 mM dithiothreitol, 2 mM $MgCl_2$, and 40 μM phalloidin. In each experiment actin was mixed with troponin and tropomyosin in a 1:1:1 molar ratio to insure saturation of actin at the low concentrations used for binding studies.

Equilibrium binding measurements

The equilibrium binding of myosin-S1 to actin-tropomyosin-troponin was determined by the decrease in phalloidin-stabilized pyrene-labeled actin fluorescence that occurs with S1 binding (Dancker et al., 1975; Kouyama and Mihashi, 1981; Criddle et al., 1985). The procedure used was essentially that described by others (Tobacman and Butters, 2000). Fluorescence measurements were made in a Spex Fluorolog fluorescence spectrophotometer (Spex Industries, Edison, NJ) with a cell maintained at 25°C with a circulating water bath. Pyrene fluorescence was measured at 384 nm with excitation at 364 nm. To reduce scattered light the 0.5-mm slits were used during the measurements. Each data point was the average of a 5-s data collection interval.

Binding experiments were done in a solution containing 20 mM MOPS pH 7.0, 110 mM KCl, 5 mM $MgCl_2$, 1 mM dithiothreitol, 2 mM ADP, 0.2 mg/ml bovine serum albumin, sufficient KCl to reach the target ionic strength, and Ca-EGTA to reach the desired pCa. The actin concentration in binding experiments was either 75 nM (at 120 mM ionic strength) or 150 nM. The solution also contained 14 units/ml hexokinase and 1 mM glucose to scavenge ATP and 20 μM Ap5A to inhibit ATP formation through the myokinase reaction. Ca-EGTA buffers were used to fix the free Ca^{2+} concentration (Fabiato and Fabiato, 1979). Ca^{2+}-EGTA was mixed with EGTA in ratios as follows (in mM) 0:2, 0.8:1.2, 1:1, 1.4:0.6, 1.8:0.2, 2:0, and the highest free Ca^{2+} concentration was obtained by using 0.1 mM $CaCl_2$ without EGTA. The free Ca^{2+} content in the solution was verified by a Corning Ca^{2+}-sensitive electrode (Corning, NY) with a Fisher Scientific AccuMet pH meter (Hampton, NH), which gave ~0, 0.6, 3, 10.3, 16.75, 20, and 70 μM free Ca^{2+}, respectively.

Titrations were done by first measuring the fluorescence of a 2-ml volume of pyrene-labeled actin-tropomyosin-troponin. A small volume of a concentrated S1 stock was added to the reaction mixture in a stirred cuvette; the sample was allowed to equilibrate for at least 5 min before measuring the fluorescence. It was important to make each measurement only after the signal had stabilized so that the constants determined were equilibrium values. The sample was exposed to incident light only during the period of observation. The fluorescence intensity and the concentration of all proteins were corrected for the volume change caused by adding S1. The total volume change for an entire binding isotherm was <10%.

Values of θ (S1 bound to actin total ratio) and free S1 concentration were calculated using the equations:

$$\theta = \frac{F_{\max} - F_i}{F_{\max} - F_{\min}}$$
$$[FreeS1] = [S1]_{\text{total}} - \theta * [Actin]_{\text{total}},$$

where F_i is the fluorescence intensity at a total S1 concentration of $i - \mu$M; $F_{\max}$ and $F_{\min}$ are the maximum and minimum values of fluorescence, respectively.

The Hill model of cooperative equilibrium binding was fitted to the binding curves (Hill et al., 1980). A long actin filament saturated with troponin and tropomyosin can be in either state 1 with low affinity for S1-ADP given by K_1 or in state 2 with a higher affinity given by K_2. Each unit of seven actin sites and one tropomyosin-troponin changes state as a group. This together with interactions between tandem groups gives rise to cooperativity. The saturation of actin with S1 (θ) as a function of free S1 concentration can be described as follows (Hill et al., 1980):

$$\left.\begin{aligned}
&\theta = p_1\theta_1 + p_2\theta_2\\
&\theta_i = \frac{K_iC}{1+K_iC}\\
&p_1 = 1 - p_2\\
&p_2 = \frac{2a}{Y\left[\sqrt{(1-a)^2 + 4\frac{a}{Y}}\left[1 - a + \sqrt{(1-a)^2 + 4\frac{a}{Y}}\right]\right]}\\
&a = \frac{(1+K_2C)^n}{(1+K_1C)^n}\frac{Y_{22}(\rho)}{LY_{11}(\rho)}\\
&L' = \frac{LY_{11}(\rho)}{Y_{22}(\rho)}\\
&Y = \frac{Y_{11}(\rho)Y_{22}(\rho)}{Y_{12}(\rho)Y_{21}(\rho)}\\
&Y_{ij}(\rho) = x_{ij} + 2k_a\rho y_{ij} + k_b^2\rho^2 z_{ij}
\end{aligned}\right\}, \quad (1)$$

with the following definitions for above set of equations (Eq. 1): p_i, fraction of actin units in i state; θ_i, fraction of actin units in the i state occupied by S1; $K_{1,2}$,constants for S1-actin binding; C, free S1 concentration; n, number of actin monomers in one actin-tropomyosin-troponin unit (assumed to be 7); L, is the equilibrium constant for transition of an isolated actin-tropomyosin-troponin unit with no neighbors, no bound Ca^{2+}, and no bound S1 from state 2 to state 1; Y, the overall cooperativity parameter; Y_{ij}, individual cooperativities between units in states i and j ($Y_{ij} = Y_{ji}$ was assumed for symmetrical case), x_{ij}, y_{ij}, and z_{ij} represent the free energy of nearest-neighbor tropomyosin interactions (W_{ij}) in exponential form $e^{-Wij/kT}$ (Hill et al., 1980), $k_{a,b}$, affinity of Ca^{2+} for troponin in states 1 and 2 with values of $\sim 10^5$ and 10^6 M^{-1}, respectively (Zot and Potter, 1987), and ρ is the free Ca^{2+} concentration. We assumed that the values of $k_{a,b}$ did not change over the ionic strength range in this study. The simulated curves were not very sensitive to the value of K_1, so simulations were normally carried out with the assumption that $K_1 = K_2/8$ (Greene and Eisenberg, 1988). However, values of K_1 less than this gave similar results.

We used the MLAB modeling system (Civilized Software, Bethesda, MD) to produce a global fit of the Hill model to all data collected at a single ionic strength condition but at varied Ca^{2+} concentrations. Because the pyrene fluorescence change monitors only the second step of the two-step binding of S1-ADP to actin the term (θ_2*p_2) of the Hill model was fitted to the fluorescence data. The constants x_{ij}, y_{ij}, z_{ij}, L, and K_2 were allowed to float to reach a best global fit. $Y(\rho)$ and $L'(\rho)$ were then calculated from the results of the fit using formulas for $Y(\rho)$ and $L'(\rho)$ from the set of equations (Eq. 1). Parameters of the fit, i.e., L, $L'(\rho) = LY_{11}(\rho)/LY_{22}(\rho)$, $Y(\rho)$, and K_2 (where L' is equilibrium constant for transition between states for the entire actin filament with Ca^{2+}, but without S1) at different ionic strengths and free Ca^{2+} concentrations were used for further mathematical simulations.

In doing a global fit it is possible to limit the predictions of the model by placing constraints on various parameters. It is common to limit the value of the cooperativity parameter Y to values >1 thus giving positive cooperativity. In this special case we constrained Y to be >1 by constraining x_{ij}, y_{ij}, z_{ij}, to values >0 and by constraining $x_{ii} > x_{ij}$, $y_{ii} > y_{ij}$, $z_{ii} > z_{ij}$. We also examined the more general case where nearest-neighbor interactions could be both favorable and unfavorable by allowing Y to be any value >0. The two fitting procedures gave identical results at physiological ionic strength or lower although a slightly better fit was obtained at higher ionic strength with negative cooperativity.

The McKillop and Geeves model (McKillop and Geeves, 1993) was also fitted to our experimental equilibrium binding curves. In this model each unit of seven actins and one tropomyosin-troponin can exist in three states. In the blocked state myosin-S1 cannot bind to actin. Binding can occur in the closed state with an equilibrium constant K_1^G but the isomerization resulting in force production cannot occur. Note that a superscript G is used to distinguish the Geeves parameter from the Hill parameter. Binding of S1 to actin in the open state occurs in two steps with equilibrium constants K_1^G and K_2^G. The transition described by K_2^G is thought to be associated with the force producing conformational change. The transitions from blocked to closed and closed to open occur with equilibrium constants K_b (or [closed]/[blocked]) and K_t (or [open]/[closed]). Binding in this case is described by the equations as follows (McKillop and Geeves, 1993):

$$R(c) = \frac{K_1^G cP^{n-1}[K_t(1+K_2^G)^n + 1]}{(K_tP^n + Q^n + 1/K_b)(1+K_2^G)^{n-1}},$$

where $P = 1 + K_1^G c(1 + K_2^G)$, $Q = 1 + K_1^G c$, n is the size of the cooperative unit, and c is the free [S1].

This equation was fitted to our experimental data to evaluate the constants K_1^G, K_2^G, K_b,and K_t.

Fitting with the McKillop and Geeves model was more complex because many combinations of parameter values could describe the equilibrium and kinetic data. Curve fitting was possible only after the values of some parameters were restricted as described earlier (McKillop and Geeves, 1991). We restricted K_b to be <10 and set $K_2^G = 20$ so this was excluded from the fit. Our fitting procedure was different from that described earlier in that we varied several parameters simultaneously. We used the kinetics of binding to determine the value of $K_b + K_b \times K_t$ in the absence of Ca^{2+}. K_b and K_t at other Ca^{2+} concentrations were allowed to float.

Binding kinetics

Rates of binding of S1 to pyrene-labeled actin were measured under the conditions used for equilibrium binding using a DX17.MV/2 sequential stopped flow spectrofluorometer (Applied Photophysics, Leatherhead, UK). The excitation wavelength was set at 364 with a monochrometer with 0.5-mm slits. Emission was measured through a 384-nm long-pass filter. All measurements were made at 25°C. Experiments were performed with either

actin or S1 in excess of actin and S1, i.e., 0.5 μM actin and 2.5 μM S1, or 2.5 μM actin and 0.5 μM S1. Unless otherwise stated, the values of concentrations given are those at the instant after mixing in the stopped flow. For further analysis and comparison with computer simulations the maximum fluorescence changes were normalized to unity.

Theoretical binding curves were calculated from the equilibrium parameters using the procedure described earlier (Chen et al., 2001). K_1 and K_2 (see above) are the equilibrium binding constants of S1-ADP to the inactive and active states of actin, respectively. The corresponding rate constants describing the two-step S1 binding and dissociation are k_1, k_1', k_2, k_2' where the apostrophe indicates the reverse rate constant. L is the equilibrium constant for transition of an isolated actin-tropomyosin-troponin from the active state to the inactive state. The rates of transition of the actin filament are α_m and β_m, where m is the number of S1 bound to the actin-tropomyosin-troponin unit (from 0 to 7). For one unit we have:

$$K_1 = \frac{k_1}{k_1'}, \quad K_2 = \frac{k_2}{k_2'}$$

$$L_m = \frac{\beta_m}{\alpha_m} = \frac{\beta_0}{\alpha_0}\left[\frac{K1}{K2}\right]^m = L\left[\frac{K1}{K2}\right]^m.$$

It can be assumed that

$$\alpha_m = \alpha_0\left[\frac{K1}{K2}\right]^{m(\gamma-1)}, \quad \beta_m = \beta_0\left[\frac{K1}{K2}\right]^{m\gamma},$$

where γ represents how $(K_1/K_2)^m$ is partitioned between α and β.

When cooperativity is present, the values of α and β can be expressed with respect to parameters from equilibrium binding (Chen et al., 2001):

$$\overline{\alpha}_m = \alpha_m\left(\frac{L'}{L}Y^{(N_1-1)}\right)^{(\delta-1)}, \quad \overline{\beta}_m = \beta_m\left(\frac{L'}{L}Y^{(N_1-1)}\right)^{\delta},$$

where N_1 (= 0, 1, 2) is the number of the two neighboring units that are in state 1, δ is a constant between 0 and 1, Y, L', K_1, K_2 describe the equilibrium binding. α_0 can be calculated from L, because $L = \beta_0/\alpha_0$, and the limits for β_0 have been chosen from earlier simulations (Brenner and Chalovich, 1999). β_0 was set near 3 at all ionic strengths and α_0 was changed in proportion to L. The other unknown parameters, k_1', k_2', δ, and γ were taken from our earlier simulations (Chen et al., 2001) with some modifications. The code for the Monte Carlo simulations was written in C++ by Dr. Bo Yan of the Mathematical Research Branch in the National Institute of Diabetes, Digestive and Kidney Diseases, National Institutes of Health.

RESULTS

Equilibrium binding

Curves for the binding of S1 to regulated actin with increasing S1 concentrations are sigmoidal indicating that there is a transition between multiple forms of the regulated actin complex. The binding is sensitive to changes in ionic strength because of direct changes in the actin-S1 interaction and also because of possible changes in the regulatory proteins. Ca^{2+} affects the distribution between the different forms of regulated actin and may have other effects. These changes were evaluated by measuring binding isotherms at a series of values of ionic strength and free Ca^{2+} concentration.

Fig. 2 shows θ, the fraction of actin sites bound to S1, as a function of the free S1 concentration at 120, 180, 225, 260, 300, and 375 mM ionic strength and at several free Ca^{2+} concentrations. Binding was measured in the presence of ADP to produce an activating state of S1 that would stabilize the active state of regulated actin. The high S1 concentration region of the curves was generally omitted from the figure so that the cooperativity is visible. Examples of full binding curves are shown as insets. At low free Ca^{2+} concentrations the curves exhibit the characteristic S shape signifying positive cooperativity. At high free Ca^{2+}, the curves appear hyperbolic. Increasing ionic strength weakens the binding so that saturation occurs at progressively higher free S1 concentrations. A more quantitative evaluation of the effects of varying the conditions was obtained by fitting the Hill model to the data.

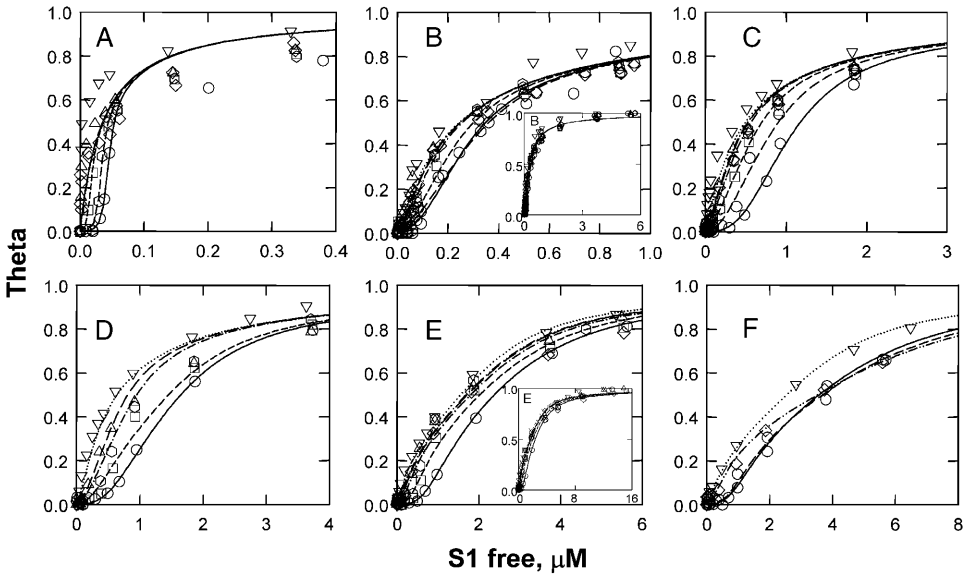

FIGURE 2 Equilibrium isotherms of S1●ADP binding to actin-tropomyosin-troponin at 120 (*A*), 180 (*B*), 225 (*C*), 260 (*D*), 300 (*E*), and 375 (*F*) mM ionic strength. In each case binding was measured at different free Ca^{2+} concentrations. The solid lines are global fits to all data at a given ionic strength. The free Ca^{2+} concentrations used at 260 and 375 mM ionic strength were 0, 3, 10, 17, 70, and 0, 0.6, 20, 70 μM going from the lower curve to the upper curve in each series. At all other ionic strengths the free Ca^{2+} concentrations were 0, 0.6, 3, 10.3, 16.75, 20, and 70 μM Ca^{2+}. Parameters from analyses of these data are given in Figs. 3 and 4. Insets show examples of complete binding curves that saturate at $\theta = 1$.

In the Hill model, the values of K_1 and K_2 are not Ca^{2+} dependent but they are dependent on the ionic strength. Therefore, we used a global fit of all data collected at the same ionic strength irrespective of the free Ca^{2+} concentration. The values of the parameters except K_1 and K_2 were allowed to float independently. The same values for K_1 and K_2 were used for all curves at a single ionic strength. The fitting was not sensitive to the value of K_1 but was highly sensitive to the value of K_2. Fig. 3 gives the ionic strength dependencies of K_2 and L obtained from the global fits. Fig. 3 *B* shows that K_2 decreased with increasing ionic strength. Values of L and K_2 were calculated with both $Y > 0$ (*squares*) and $Y > 1$ (*circles*) where only positive cooperativity was permitted (Fig. 3). Restrictions on the value of Y had little effect on either parameter.

Values of $L'(\rho)$ and $Y(\rho)$ were calculated from Eq. 1 assuming that the affinity of troponin for Ca^{2+} was independent of ionic strength. The results are shown in Fig. 4. Fig. 4, *A* and *B*, show the results that were obtained if both positive and negative cooperativity were allowed. Fig. 4, *C* and *D*, are the corresponding results when Y was restricted to values giving positive cooperativity ($Y > 1$). The cooperativity parameter, Y, increased with increasing Ca^{2+} concentrations at ionic strengths from 120 to 260 mM. At higher ionic strength the cooperativity decreased with increasing Ca^{2+} to give negative cooperativity (Fig. 4 *A*) unless constrained (Fig. 4 *C*). At the intermediate ionic strength values used, the value of Y was approximately independent of Ca^{2+}. When Y was unconstrained the value of L' decreased with increasing Ca^{2+} concentrations and increased with increasing ionic strength (Fig. 4 *B*). That is, whereas Ca^{2+} stabilized the active state (state 2), increases in ionic strength at any Ca^{2+} concentration tended to stabilize the inactive state (state 1). When the value of Y was limited to values >1 the values of L' at the highest ionic strengths were decreased at all values of Ca^{2+}. This resulted in a more narrow distribution of values of L' as shown in Fig. 4 *D*.

Little information is available about the salt dependence of the binding of Ca^{2+} to actin-tropomyosin-troponin in both the inactive and active states. We assumed that the affinity for Ca^{2+} did not depend on the ionic strength. In the case of pure troponin C the affinity at 300 mM ionic strength is ~0.5 that at 120 mM (Ogawa, 1985; Iida, 1988). We repeated the fitting of the 300-mM ionic strength binding curve assuming that the affinity decreased by an even larger fraction to 0.2 of the value at 120 mM ionic strength. The values of the binding parameters at 300 mM ionic strength changed slightly when the Ca^{2+} affinity was assumed to be lower. In the absence of Ca^{2+} the values of Y and L' were 10% smaller than with the higher Ca^{2+} affinity. At saturating Ca^{2+} the values of Y and L' were 10% higher than with the higher Ca^{2+} affinity. That is, with the assumption of a decreased Ca^{2+} affinity at high ionic strength the relationship of Y and L' was slightly flattened out. Because the data of Fig. 4 *B* are on a log scale the change resulting from this assumption was small.

Binding kinetics

We recently demonstrated the feasibility of simulating the kinetics of S1 binding to regulated actin based on the parameters obtained from equilibrium binding using the Hill model (Chen et al., 2001). The kinetics of binding are ionic strength dependent with a nonlinear relationship between the duration of the lag in binding and the ionic strength (Resetar et al., 2002). Simulation of binding kinetics from equilibrium binding parameters (L, L', Y, K_2) at several different ionic strength conditions provides a robust test of the model.

Several examples of the observed kinetic traces of S1-ADP binding to regulated actin and the theoretical curves are shown in Fig. 5. Fig. 5, *A* and *B*, show changes in pyrene actin fluorescence as a function of time with S1 in excess over actin. Binding in the presence of Ca^{2+} (Fig. 5 *B*) occurred with ~10 times the rate as that in the absence of Ca^{2+} (Fig. 5 *A*). Binding in the absence of Ca^{2+} is initially slow but the rate increases with time. This gives rise to a lag in the binding in the absence of Ca^{2+} that is often explained by a large fraction of regulated actin that is blocked by tropomyosin so that S1-ADP cannot bind. In this blocked state model S1-ADP binding to available sites results in a cooperative decrease in the population of blocked regulated actin so that the rate of binding increases. The theoretical curves calculated from our equilibrium binding parameters show the same trends that were found experimentally without the inclusion of a blocked state.

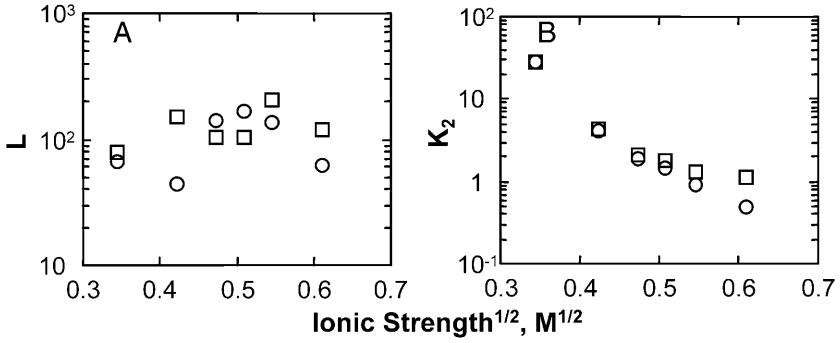

FIGURE 3 Dependencies of equilibrium binding parameters from the Hill model on the square root of the ionic strength. (*A*) L is the equilibrium constant for transition of an isolated actin-tropomyosin-troponin unit with no neighbors, no bound Ca^{2+}, and no bound S1 from state 2 to state 1. (*B*) K_2 is the affinity of S1-ADP for regulated actin in state 2. Squares show parameters obtained by assuming that $x, y, z > 0$ (i.e., $Y > 0$). Circles show parameters obtained by assuming that $x_{ii} > x_{ij}$, $y_{ii} > y_{ij}$, $z_{ii} > z_{ij}$ (i.e., $Y > 1$, no negative cooperativity). Both L and K_2 are Ca^{2+} independent. Both ordinates are on a log scale.

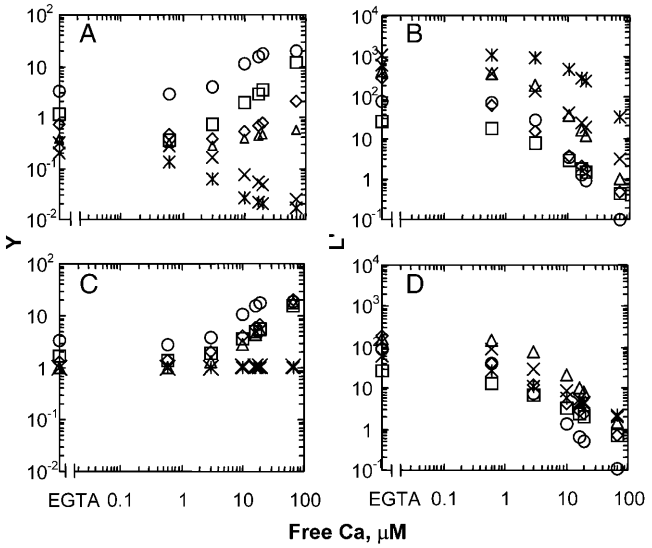

FIGURE 4 Calcium dependence of the Hill model parameters for equilibrium binding of S1-ADP to actin-tropomyosin-troponin. (*A*) Y is the cooperativity parameter. (*B*) L' is the equilibrium constant for transition between states for the entire regulated actin filament with Ca^{2+}, but without S1. (*C* and *D*) The same parameters as in *A* and *B* but obtained, as described in the above figure, assuming $Y > 1$. Ionic strength was 120 mM (○); 180 mM (□); 225 mM (◇); 260 mM (△); 300 mM (×); and 375 mM (*). Both axes are on a log scale.

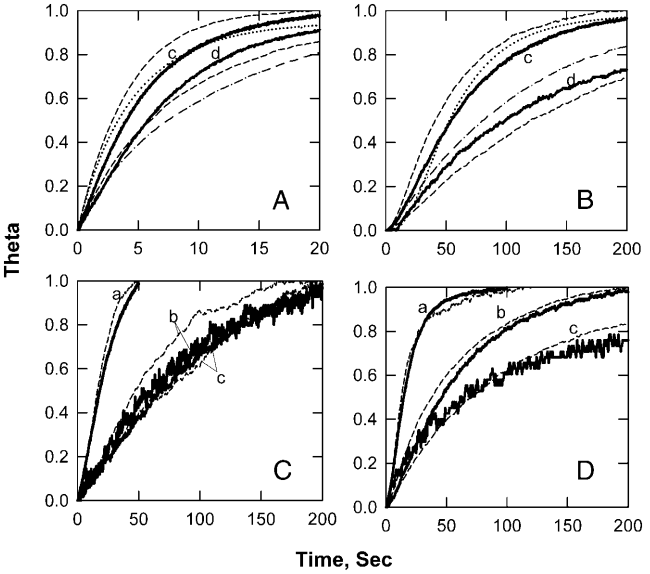

FIGURE 5 Examples of simulations of the rate of binding of S1-ADP to actin-tropomyosin-troponin. Data shown as solid lines are pyrene fluorescence values at different times after mixing. In all cases, the maximum value of fluorescence was defined as 1. Curves *a–d* represent 120, 180, 225, and 300 mM ionic strength, respectively. Panels *A* and *B* show 2.5 μM S1 binding to 0.5 μM actin-tropomyosin-troponin at high Ca^{2+} (70 μM) (*A*) and in the presence of 2 mM EGTA (*B*); panels *C* and *D* represent 2.5 μM actin-tropomyosin-troponin and 0.5 μM S1 binding at high Ca^{2+} (*C*) and in 2mM EGTA (*D*) superimposed with computer simulations of binding. Dashed lines are fits of the Hill model to the data using parameters from equilibrium measurements. The dotted lines show binding rates obtained from fitting the McKillop and Geeves model to data obtained at 225 mM ionic strength (parameters of the fit are in Table 2). The dashed-dotted line shows rates simulated by applying the Hill model to equilibrium binding at 300 mM ionic strength assuming $Y > 1$.

Fig. 5, *C* and *D*, show the other case of binding where the actin concentration was in excess over S1. The decreased rate in binding in the absence of Ca^{2+} is normally explained on the basis of a fraction of regulated actin that is blocked by tropomyosin so that binding cannot occur. This has the effect of decreasing the concentration of actin available for reaction. Examples of theoretical time courses are shown that were calculated using the Hill model and constants determined from equilibrium binding experiments. Despite the absence of a blocked state in this model there is good agreement with the experimental curves despite inevitable experimental errors in both the equilibrium and kinetic measurements.

The kinetics of binding could be simulated using equilibrium binding values from an unconstrained fit as well as with the constraint of positive cooperativity ($Y > 1$). In the unconstrained case negative cooperativity occurred in EGTA when the ionic strength was at 225 mM or greater and in Ca^{2+} when the ionic strength was 260 mM or greater. Examples of a simulation at high ionic strength (300 mM) with the constraint of positive cooperativity are shown in Fig. 5, *A* and *B* (*dashed-dotted line* near curve *d*). The fits are reasonable in this case but the value of β, the rate constant from the inactive state to the active state had to be reduced three times to obtain a good fit. It was impossible to decide between the two cases ($Y > 0$ and $Y > 1$) on the basis of fitting either the equilibrium binding or kinetic data.

Table 1 summarizes the values of the parameters used to simulate both equilibrium binding and binding kinetics from 120 to 375 mM ionic strength at both saturating Ca^{2+} and in the virtual absence of Ca^{2+}.

Fig. 5, *A* and *B* (*dotted curves c*), shows a fit of the McKillop and Geeves model to the curve for binding 2.5 μM [S1] to 0.5 μM regulated actin. These curves are the best fits of the model to the curves shown (see Table 2 legend). This is in contrast to the curves shown for the Hill model where the same parameters were used for all curves.

We showed previously that the duration of the lag in binding increased with increasing ionic strength even beyond physiological values of ionic strength (Resetar et al., 2002). However, we did not know the reason for this increased lag. Fig. 6 compares the lag duration from the experimental time courses with those obtained from simulations in Fig. 5. As in our earlier data the lag duration increased with ionic strength. It is also apparent from Fig. 6 that the simulations accurately predicted the lag duration. That means that the increased lag may be attributed largely to the increased stability of the inactive state of regulated actin, state 1.

We also fitted the McKillop and Geeves model to some of the equilibrium binding curves shown in Fig. 2. Curve fitting

TABLE 1 Parameters of equilibrium binding and constants used to simulate binding kinetics

	Ionic strength											
	120 mM		180 mM		225 mM		260 mM		300 mM		375mM	
	Ca	EGTA	Ca	EGTA	Ca	EGTA	Ca	EGTA	Ca	EGTA	Ca	EGTA
L'	0.1	70.6	1.0	126	0.47	299	0.98	439	3.2	645	32.5	1125
Y	19.2	3.3	11.4	1.16	1.99	0.72	0.55	0.39	0.025	0.32	0.02	0.2
L	78		150		103		102		204		116	
K_2	28.5×10^6		4.1×10^6		2×10^6		1.7×10^6		1.3×10^6		1.1×10^6	
$k'_{1(Ac<S1)}$	4	0.04	–	–	–	–	–	–	–	–	–	–
$k'_{1(Ac>S1)}$	0.03	4×10^{-4}	–	–	–	–	–	–	–	–	–	–
$k'_{2(Ac<S1)}$	0.09	0.09	–	–	–	–	–	–	–	–	–	–
$k'_{2(Ac>S1)}$	9×10^{-4}	0.09	–	–	–	–	–	–	–	–	–	–
β_0	3											
γ	0.95											
δ	0.5											

without restrictions on the parameters was not possible because there was no unique set of parameters defining the fit. By restricting some parameters in accord with the McKillop and Geeves model we were able to find the best fit of remaining parameters as shown in Fig. 7 *A*. These parameters may be compared to those of McKillop and Geeves based on their data collected under similar conditions (Fig. 7 *B*). We limited our analysis to a single ionic strength condition that was similar to that used by Maytum et al. (1999). Our analysis produced a steeper increase in both K_b and K_t with increasing free calcium than shown in their Fig. 7 *B*. Furthermore the value of n decreased with increasing free Ca^{2+} in our analysis whereas n increased in their Fig. 7 *B*. The parameters for the McKillop and Geeves model are given in Table 2.

TABLE 2 Parameters of the McKillop and Geeves model at 225 mM ionic strength

Ca, μM	K_2	$K_1 \times 10^4$	K_b	K_t	n
0	20/20*	5.7/1.1*	0.495/0.43*	0.011/0.004*	9.2/7*
0.6	–	9.1	2.4	0.065	4.9
3	–	18	2.4	0.26	1.8
10	–	23.4	5	0.17	1.9
17	–	21.7	1.27	0.64	1.4
20	–	12.3	4.7	1.04	1.6
70	–/–*	19.8/10.6*	10/8.9*	2.68/18.8*	0.73/1*

*Parameters obtained by using the procedure of Chen et al. (2001) for fitting the McKillop and Geeves model to kinetics data obtained at 225 mM ionic strength (see Fig. 5, *A* and *B*). Binding rate parameters used for fit were constrained by values obtained from fitting equilibrium binding isotherms. K_2 was fixed at 20. The size of cooperative unit, n, stipulates the number of states in the kinetic diagram. For example in the model (Chen et al., 2001) for $n = 7$ there will be 45 states and for $n = 1$ there are six states. The value of n was set indirectly by the number of differential equations used in the analysis. For binding in Ca^{2+} $n = 1$ and six equations were used. For EGTA, although $n = 9$, we could not fit 64 equations but as an approximation used 45 differential equations, the number for the $n = 7$ case. The remaining parameters were obtained by fitting the McKillop and Geeves model (1993) to equilibrium binding data shown in Fig. 2 *C*.

DISCUSSION

The tropomyosin-troponin regulatory system makes the force producing interaction between actin and myosin sensitive both to Ca^{2+} and the saturation of actin with myosin. This system may be fine tuned by changes in the level of phosphorylation of troponin I and troponin T (Noland and Kuo, 1993) or by changes in the expression of troponin isoforms (Anderson et al., 1991). Seemingly small changes in the primary structure of troponin I or troponin T result in disorders including myopathies (Braun et al., 1996; Nowak et al., 1999) and cardiomyopathies (Thierfelder et al., 1994). Our goal is to provide a framework for studying these adaptive and pathologic changes. We propose that changes in the binding of tropomyosin-troponin to actin result in the formation of multiple parallel pathways with different rates of ATP hydrolysis. Ca^{2+} and myosin act as effectors that stabilize the active state of regulated actin (Fig. 1).

This view was based on observations that the binding of myosin to regulated actin during steady-state hydrolysis of

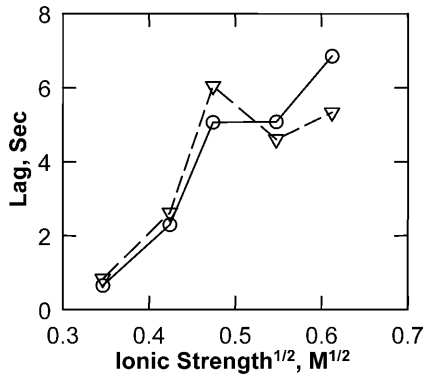

FIGURE 6 Ionic strength dependence of a lag of binding kinetics of S1 and actin-tropomyosin-troponin. Triangles represent the lag estimated by the experiment binding kinetics obtained at different ionic strength (120–375 mM) in the solution containing 2 mM EGTA. Circles show the lag predicted by the Hill's simulations of binding kinetics.

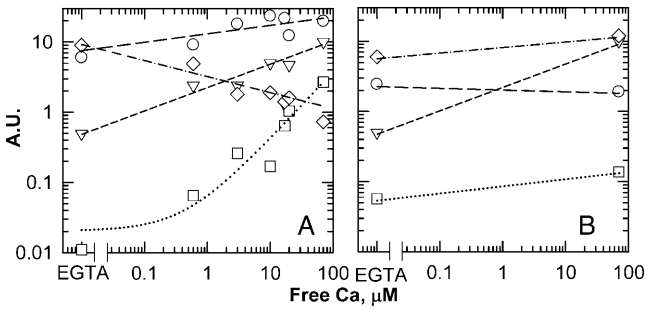

FIGURE 7 Parameters of the McKillop and Geeves model. (*A*) Parameter values for the equilibrium binding data of Fig. 2 *C* for titration of 75 nM actin-tropomyosin-troponin with S1 in the solution containing 208 mM KCl, 2 mM ADP, 5 mM $MgCl_2$, 1 mM glucose, 20 μM Ap_5A, 14 units/ml hexokinase, 0.2 mg/ml bovine serum albumin, 1 mM dithiothreitol, and 20 mM MOPS, pH 7. Free Ca^{2+} was varied from nearly 0 to 70 μM. The fitting procedure is explained in the text. The value of K_2 was fixed at 20, K_b was limited to values <10, and the sum of $K_b(1 + K_t)$ in the absence of Ca^{2+} was set to 1/2 to be consistent with binding kinetics (Fig. 5). The final fitted parameters are dependent on these restrictions. (*B*) Previously published parameters (Maytum et al., 1999) for titration of 50 nM actin-tropomyosin-troponin with S1 in the solution containing 200 mM KCl, 2 mM ADP, 50 μM Ap_5A, 1 mM glucose, 2.5 units of hexokinase, 5 mM $MgCl_2$, 20 mM MOPS, pH 7. n ($\diamond$); $K_1 \times 10^4$ ($\circ$); K_t ($\square$); and K_b ($\triangledown$).

ATP is not greatly affected by Ca^{2+} (Chalovich et al., 1981; Brenner et al., 1982; Resetar et al., 2002), that the increase in ATPase rate in response to Ca^{2+} results from an increase in the k_{cat} (see Chalovich, 1992), and that the mode of interaction between myosin and regulated actin can be classified into two states depending on the nucleotide bound to myosin (Chalovich, 1992; Brenner and Chalovich, 1999). Thus S1-ADP (but not S1-ATP) binding to regulated actin is cooperative with increasing S1 concentration and the binding is also somewhat enhanced by Ca^{2+}. The parallel pathway model could simulate the equilibrium binding of S1 and S1-ADP to regulated actin (Hill et al., 1980) and the general features of the steady-state ATPase activity (Hill et al., 1981). However the inclusion of an additional state was thought to be required to explain binding kinetics (Trybus and Taylor, 1980; McKillop and Geeves, 1993). The effect of Ca^{2+} on binding kinetics was used to define the fraction of regulated actin in that additional state, the blocked state (Head et al., 1995). A subsequent analysis showed that the two-state Hill model gave the same predictions of binding kinetics as a model including a blocked state (Chen et al., 2001).

We now show that the Hill model could simulate equilibrium binding of S1-ADP to regulated actin and the kinetics of binding at several ionic strengths and over a range of free Ca^{2+} concentrations. All equilibrium binding data at a single ionic strength were analyzed globally so that all curves within a series could be predicted just by varying the free Ca^{2+} concentration. The resulting binding parameters could be used to simulate the rate of binding of S1-ADP to actin-tropomyosin-troponin both with actin in excess over S1 and with S1 in excess over actin. In the latter case the binding rate increased with time as the regulated actin filament became increasingly more active as S1-ADP stabilized the active state. The two-state version of the Hill model can describe binding kinetics in addition to the equilibrium binding and ATPase activities that were analyzed earlier (Hill et al., 1980, 1981).

We also evaluated our 225-mM ionic strength data using the McKillop and Geeves model. Our fitted values differ from published data obtained under similar conditions (Maytum et al., 1999) in several respects as shown in Fig. 7. In both cases K_b and K_t increase with increasing free Ca^{2+} concentration but our analysis of our data gave lower values of K_t in the absence of Ca^{2+} and our curve increased more steeply with increasing Ca^{2+} than does their curve (Maytum et al., 1999). We found that K_1 is higher than they reported and our value increased slightly with Ca^{2+} whereas theirs decreased slightly. Similarly, we find that the value of n, the size of the cooperative unit, decreased with Ca^{2+} whereas they found higher values of n that increased with increasing Ca^{2+} (Geeves and Lehrer, 1994). These effects should be considered when rationalizing the physical significance of n.

The reasons for the different values in Fig. 7 are both experimental and analytical. Our equilibrium titrations were done over a much longer time course to ensure that each measurement reported an equilibrium value. In fitting the model to data we reduced the number of fixed parameters and simultaneously minimized the errors of all remaining parameters.

Previous examinations of the blocked state model were done by letting K_1 and K_t float with fixed values of K_b and K_2 (Maytum et al., 1999). The value of n was assumed to be an integer between 5 and 15. Values of n giving the minimum least-square difference were used in subsequent modeling. That value was different at low and high free Ca^{2+}. The value of K_b was assumed to be >10 in the presence of Ca^{2+} and was excluded from the fit. In the absence of Ca^{2+} the value of K_b was estimated from the ratio of binding rates in the absence (k_{-Ca}) and presence (k_{+Ca}) of Ca^{2+}. The assumption was made that the reduction in rate was due to a decrease in available actin concentration as a result of steric blocking. Then K_b was calculated using the formula $k_{-Ca}/k_{+Ca} = 1 - 1/(1 + K_b(1 + K_t))$ with the assumption that $K_t = 0$. The fitting algorithm was repeated with this value of K_b to find the best values of K_1 and a new value of K_t. The value of n was optimized by exploring integers between 5 and 15. The new value of K_t was usually smaller than that in the presence of Ca^{2+}. The final results are not a universal solution because of the indeterminate uncertainty in K_t.

We attempted to improve this fitting procedure but we could not avoid fixing some parameters. In accord with previous simulations (Maytum et al., 1999) we set $K_2 = 20$ and restricted K_b between 0 and 10. Likewise, we assumed that in the presence of Ca^{2+} there was no blocked state. In the absence of Ca^{2+} the value of K_b was determined from the equation $k_{-Ca}/k_{+Ca} = 1 - 1/(1 + K_b(1 + K_t))$ (Maytum et al., 1999). In this case $k_{-Ca}/k_{+Ca} = 1/3$, so $K_b(1 + K_t) = 1/2$. At

this point our modeling differed. We did not fix K_b by assuming a value of K_t; rather, we allowed the MLAB fitting routine to obtain the best values of K_t, K_b, n, and K_1 taking into account the above-mentioned equation. The constraint that $K_b(1 + K_t) = 1/2$ was relaxed when the Ca^{2+} concentration was elevated although $K_b(1 + K_t)$ appeared to be $>1/2$ at all free Ca^{2+} concentrations.

The blocked state model has a great deal of flexibility in the parameters and a large sensitivity to the initial assumptions. When fitting multiple parameters simultaneously, as we have done, the fit was not highly sensitive to the value of n. Also, values of K_b and K_t could largely compensate for each other so that it was difficult to determine which parameter was more sensitive to Ca^{2+} and of greatest regulatory importance. It is possible that Ca^{2+} may have a larger effect on K_t than previously thought. In that case, like the Hill model, the major regulatory event would be a transition between two bound states rather than a change in binding. It is known experimentally that Ca^{2+} has a large effect on the k_{cat} of regulated actin-activated ATPase activity (King and Greene, 1985; Wagner, 1984; El-Saleh and Potter, 1985; Chalovich and Eisenberg, 1982) and the large effect on the rate of product release (Heeley et al., 2002). Such large effects require a change in the rate of transition between two bound states.

Earlier studies of the kinetics of binding of S1 to regulated actin reported that the effect of Ca^{2+} on the rate of binding did not occur at ionic strengths below 50 mM (Head et al., 1995). Because the reduction in the rate of binding at low Ca^{2+} was assumed to result from a fraction of regulated actin that could not bind to S1 this observation led to the proposal that the blocked state exists only above 50 mM ionic strength. A later study showed that the Ca^{2+} sensitivity of binding was even more complex than previously thought. The lag in binding with excess S1 and no free Ca^{2+} increased in a nonlinear manner from 30 mM ionic strength to ~300 mM ionic strength (Resetar et al., 2002). We are now able to explain that effect on the basis of an increased stability of state 1 of regulated actin at high ionic strength. Fig. 6 shows that the duration of the lag in binding is well described by the salt-dependent changes in the equilibrium binding parameters.

The stabilization of state 1 with increasing salt concentration was seen as an increase in the value of L with ionic strength. L is the equilibrium constant favoring state 1 for a single regulatory unit in the absence of tropomyosin-tropomyosin interactions and without bound S1 or Ca^{2+}. The value of L' also increased with increasing ionic strength so that the inactive state becomes more stable. L' is equal to L times the ratio of the cooperativity parameters for two tropomyosin units in state 1 compared to state 2 at an arbitrary Ca^{2+} concentration, ρ. The increase in L contributes to the increase in L' with ionic strength although it is possible that the ratio $Y_{11}(\rho)/Y_{22}(\rho)$ also increases to give an overall greater salt dependence of L'. A salt effect on the ratio $Y_{11}(\rho)/Y_{22}(\rho)$ could be due either to stabilization of the interaction between adjacent tropomyosin molecules in state 1 or destabilization of adjacent tropomyosin molecules in state 2. This change is the same at high and low Ca^{2+} concentrations.

Values of Y tend to decrease as the ionic strength is increased so there is less tendency of adjacent regulatory units to be in the same state. In fact, the best fit of some data sets occurred when the value of Y was between 0 and 1, that is when there was negative cooperativity between adjacent tropomyosin molecules. It was possible to obtain almost as good of a fit if the value of Y was constrained so that negative cooperativity was impossible. In those cases, the value of Y tended to approach 1 (no cooperativity) with increasing ionic strength. The decrease in the value of Y may be related to a decrease in the end-to-end interaction of tropomyosin with increasing ionic strength. Sousa and Farah measured the linear polymerization of tropomyosin as a function of ionic strength (Sousa and Farah, 2002). At 8 μM tropomyosin the fraction polymerized was ~90% at 25 mM NaCl, and 20% at 150 mM NaCl. Beyond 200 mM NaCl there was no appreciable polymerization. This lack of coupling between tropomyosin molecules at high ionic strength would be expected to reduce the value of Y as we have observed.

Negative cooperativity could occur if steric repulsion or other repulsive forces were dominant at high ionic strength when the end-to-end interactions among tropomyosin molecules were small. Unfavorable interactions could occur at high ionic strength between adjacent tropomyosin molecules, between tropomyosin and troponin, or between other protein pairs. At this time we have no compelling argument for or against negative cooperativity at high ionic strength. The key points are that positive cooperativity occurs at physiological ionic strength and that the Hill model functions well with both assumptions over a wide range of conditions.

Several of the parameters defining equilibrium binding varried with the free Ca^{2+} concentration. The value of L' decreased with increasing Ca^{2+} as expected so that state 2 was more stable in the presence of Ca^{2+}. The Ca^{2+} dependence of Y is more complex. Below 225 mM ionic strength, the value of Y increased with increasing Ca^{2+} whereas above 260 mM ionic strength Y decreased with increasing ionic strength. There is some uncertainty in the Ca^{2+} dependence of the parameters L' and Y because of the assumption that the affinity of troponin C for Ca^{2+} is ionic strength independent. We have evaluated the binding parameters for the 300-mM ionic strength condition with the assumption that the affinity for Ca^{2+} decreased to 0.2 times the value at 120 mM ionic strength. This value was chosen because it exceeds the observed change in affinity of pure troponin C for Ca^{2+} (Ogawa, 1985; Iida, 1988). The effects of introducing a change in Ca^{2+} affinity on the parameters Y and L' were small and do not alter the conclusions.

We are unaware of models other than the Hill model that have been shown to predict ATPase activities, equilibrium binding and binding kinetics. Smith, Maytum, and Geeves have proposed a new type of regulatory model that is largely

based on available structural data (Smith et al., 2003). That model, like the earlier Geeves model, has three states of tropomyosin corresponding to the three observed positions of tropomyosin on actin (Vibert et al., 1997). That model also incorporates the idea of a flexible tropomyosin molecule so that adjacent actin protomers within the influence of a single tropomyosin molecule may exist in states having different activities. The kink size of the flexible tropomyosin was found to track the size of the cooperative unit of their earlier model. Our own evaluation of the cooperative unit (Fig. 7 or Table 2) differed from that reported by Maytum et al. (1999) and would not exhibit the same relationship. The model of Smith et al. (2003) was able to fit curves for the equilibrium binding of S1 to regulated actin in the presence and absence of Ca^{2+} (Smith and Geeves, 2003). Although the full predictive ability of that model has not been explored this is an interesting new approach.

In the original Hill model the simplifying assumption was made that the ATPase activity increased in going to state 2 but did not change in going from state 1 with no bound Ca^{2+} to state 1 with bound Ca^{2+}. Although this two-state model is sufficient to explain function in solution it will be necessary to include an additional functional state if the third observed structural state has a unique function. The Hill model can be readily expanded to three states (Fig. 1). The major states 1 and 2 can exist with either 0, 1, or 2 bound Ca^{2+} (Fig. 1). Because of the cooperativity of Ca^{2+} binding it is most likely that a regulatory unit will have either 0 or 2 bound Ca^{2+}. Therefore, the most reasonable possibilities are states 1_0, 1_2, 2_0, and 2_2. The latter two states seem to be similar if not identical in terms of their properties (Greene and Eisenberg, 1988) so that it would be quite reasonable to have three functional states, 1_0, 1_2, and 2. Treating state 1_2 as a third state would mean assigning this state with an ATPase activity intermediate between those of states 1_0 and 2. However all three states would retain the ability of binding to S1 during steady-state ATP hydrolysis; that is, none of these would be a blocked state. We have not been able to distinguish two-state and three-state models by an analysis of equilibrium binding and binding kinetics. The number of functional states may be apparent from a more detailed analysis of the effect of Ca^{2+} and ionic strength on the regulation of ATPase activity.

We thank Mr. Michael Vy-Freedman and Ms. Anmei Cai for technical assistance and Dr. Mechthild Schroeter for critical reading of this manuscript.

This work was supported by the National Institutes of Health (grant AR40540 to J.M.C.).

REFERENCES

Anderson, P. A. W., N. N. Malouf, A. E. Oakeley, E. D. Pagani, and P. D. Allen. 1991. Troponin T isoform expression in humans: a comparison among normal and failing adult heart, fetal heart, and adult and fetal skeletal muscle. *Circ. Res.* 69:1226–1233.

Braun, S. L., D. E. Pongratz, P. Bialk, S. Liem, B. Schlotter, and W. Vogt. 1996. Discrepant results for cardiac troponin T and troponin I in chronic myopathy, depending on instrument and assay generation. *Clin. Chem.* 42:2039–2041.

Brenner, B., and J. M. Chalovich. 1999. Kinetics of thin filament activation probed by fluorescence of *N*-((2- (iodoacetoxy)ethyl)-*N*-methyl)amino-7-nitrobenz-2-oxa-1, 3-diazole- labeled troponin I incorporated into skinned fibers of rabbit psoas muscle: implications for regulation of muscle contraction. *Biophys. J.* 77:2692–2708.

Brenner, B., M. Schoenberg, J. M. Chalovich, L. E. Greene, and E. Eisenberg. 1982. Evidence for cross-bridge attachment in relaxed muscle at low ionic strength. *Proc. Natl. Acad. Sci. USA.* 79:7288–7291.

Chalovich, J. M. 1992. Actin mediated regulation of muscle contraction. *Pharmacol. Ther.* 55:95–148.

Chalovich, J. M. 2002. Regulation of striated muscle contraction: a discussion. *J. Muscle Res. Cell Motil.* 23:353–361.

Chalovich, J. M., P. B. Chock, and E. Eisenberg. 1981. Mechanism of action of troponin-tropomyosin: inhibition of actomyosin ATPase activity without inhibition of myosin binding to actin. *J. Biol. Chem.* 256:575–578.

Chalovich, J. M., and E. Eisenberg. 1982. Inhibition of actomyosin ATPase activity by troponin-tropomyosin without blocking the binding of myosin to actin. *J. Biol. Chem.* 257:2432–2437.

Chen, Y., B. Yan, J. M. Chalovich, and B. Brenner. 2001. Theoretical kinetic studies of models for binding myosin subfragment-1 to regulated actin: Hill model versus Geeves model. *Biophys. J.* 80:2338–2349.

Craig, R., and W. Lehman. 2001. Crossbridge and tropomyosin positions observed in native, interacting thick and thin filaments. *J. Mol. Biol.* 311:1027–1036.

Criddle, A. H., M. A. Geeves, and T. Jeffries. 1985. The use of actin labeled with N-(1-pyrenyl)iodoacetamide to study the interaction of actin with myosin subfragments and troponin/tropomyosin. *Biochem. J.* 232: 343–349.

Dancker, P., I. Low, W. Hasselbach, and T. Wieland. 1975. Interaction of actin with phalloidin: polymerization and stabilization of F-actin. *Biochim. Biophys. Acta.* 400:407–414.

Eisenberg, E., and W. W. Kielley. 1972. Evidence for a refractory state of heavy meromyosin and subfragment-1 unable to bind to actin in the presence of ATP. *Cold Spring Harb. Symp. Quant. Biol.* 37:145–152.

Eisenberg, E., and W. W. Kielley. 1974. Troponin-tropomyosin complex. Column chromatographic separation and activity of the three active troponin components with and without tropomyosin present. *J. Biol. Chem.* 249:4742–4748.

Eisenberg, E., and R. R. Weihing. 1970. Effect of skeletal muscle native tropomyosin on the interaction of amoeba actin with heavy meromyosin. *Nature.* 228:1092–1093.

El-Saleh, S. C., and J. D. Potter. 1985. Calcium-insensitive binding of heavy meromyosin to regulated actin at physiological ionic strength. *J. Biol. Chem.* 260:14775–14779.

Fabiato, A., and F. Fabiato. 1979. Calculator programs for computing the composition of the solutions containing multiple metals and ligands used for experiments in skinned muscle cells. *J. Physiol. (Paris).* 75:463–505.

Geeves, M. A., and D. J. Halsall. 1987. Two-step ligand binding and cooperativity. A model to describe the cooperative binding of myosin subfragment 1 to regulated actin. *Biophys. J.* 52:215–220.

Geeves, M. A., and S. S. Lehrer. 1994. Dynamics of the muscle thin filament regulatory switch: the size of the cooperative unit. *Biophys. J.* 67:273–282.

Greene, L. E., and E. Eisenberg. 1980. Cooperative binding of myosin subfragment-1 to the actin-tropomyosin-troponin complex. *Proc. Natl. Acad. Sci. USA.* 77:2616–2620.

Greene, L. E., and E. Eisenberg. 1988. Relationship between regulated actomyosin ATPase activity and cooperative binding of myosin to regulated actin. *Cell Biophys.* 12:59–71.

Hai, H., K. Sano, K. Maeda, Y. Maeda, and M. Miki. 2002. Ca^{2+}- and S1-induced conformational changes of reconstituted skeletal muscle thin

filaments observed by fluorescence energy transfer spectroscopy: structural evidence for three states of thin filament. *J. Biochem. (Tokyo).* 131:407–418.

Haselgrove, J. C., and H. E. Huxley. 1973. X-ray evidence for radial cross-bridge movement and for the sliding filament model in actively contracting skeletal muscle. *J. Mol. Biol.* 77:549–568.

Head, J. G., M. D. Ritchie, and M. A. Geeves. 1995. Characterization of the equilibrium between blocked and closed states of muscle thin filaments. *Eur. J. Biochem.* 227:694–699.

Heeley, D. H., B. Belknap, and H. D. White. 2002. Mechanism of regulation of phosphate dissociation from actomyosin-ADP-Pi by thin filament proteins. *Proc. Natl. Acad. Sci. USA.* 99:16731–16736.

Hill, T. L., E. Eisenberg, and J. M. Chalovich. 1981. Theoretical models for cooperative steady-state ATPase activity of myosinsubfragment-1 on regualted actin. *Biophys. J.* 35:99–112.

Hill, T. L., E. Eisenberg, and L. E. Greene. 1980. Theoretical model for the cooperative equilibrium binding of myosinsubfragment 1 to the actin-tropomyosin-troponin complex. *Proc. Natl. Acad. Sci. USA.* 77:3186–3190.

Iida, S. 1988. Calcium binding to troponin C. II. A Ca^{2+} ion titration study with a Ca^{2+} ion sensitive electrode. *J. Biochem.* 103:482–486.

Kielley, W. W., and W. F. Harrington. 1960. A model for the myosin molecule. *Biochim. Biophys. Acta.* 41:401–421.

King, R. T., and L. E. Greene. 1985. Regulation of the adenosinetriphosphatase activity of cross-linked actin-myosin subfragment 1 by troponin-tropomyosin. *Biochemistry.* 24:7009–7014.

Kouyama, T., and K. Mihashi. 1981. Fluorimetry study of N-(1-pyrenyl)iodoacetamide-labeled F-actin: local structural change of actin protomer both on polymerization and on binding of heavy meromyosin. *Eur. J. Biochem.* 114:33–38.

Kress, M., H. Huxley, and A. R. Faruqi. 1986. Structural changes during activation of frog muscle studied by time-resolved X-ray diffraction. *J. Mol. Biol.* 188:325–342.

Maytum, R., S. S. Lehrer, and M. A. Geeves. 1999. Cooperativity and switching within the three-state model of muscle regulation. *Biochemistry.* 38:1102–1110.

McKillop, D. F. A., and M. A. Geeves. 1991. Regulation of the acto.myosin subfragment 1 interaction by troponin/tropomyosin. Evidence for control of a specific isomerization between two acto.myosin subfragment 1 states. *Biochem. J.* 279:711–718.

McKillop, D. F. A., and M. A. Geeves. 1993. Regulation of the interaction between actin and myosin subfragment 1: evidence for three states of the thin filament. *Biophys. J.* 65:693–701.

Murray, J. M., M. K. Knox, C. E. Trueblood, and A. Weber. 1982. Potentiated state of the tropomyosin actin filament and nucleotide-containing myosin subfragment 1. *Biochemistry.* 21:906–915.

Noland, T. A., Jr., and J. F. Kuo. 1993. Protein kinase C phosphorylation of cardiac troponin I and troponin T inhibits Ca^{2+}-stimulated MgATPase activity in reconstituted actomyosin and isolated myofibrils, and decreases actin-myosin interactions. *J. Mol. Cell. Cardiol.* 25:53–65.

Nowak, K. J., D. Wattanasirichaigoon, H. H. Goebel, M. Wilce, K. Pelin, K. Donner, R. L. Jacob, C. Hübner, K. Oexle, J. R. Anderson, C. M. Verity, K. N. North, S. T. Iannaccone, C. R. Müller, P. Nürnberg, F. Muntoni, C. Sewry, I. Hughes, R. Sutphen, A. G. Lacson, K. J. Swoboda, J. Vigneron, C. Wallgren-Pettersson, and A. H. Beggs. 1999. Mutations in the skeletal muscle α-actin gene in patients with actin myopathy and nemaline myopathy. *Nat. Genet.* 23:208–212.

Ogawa, Y. 1985. Calcium binding to troponin C and troponin: effects of Mg^{2+}, ionic strength and pH. *J. Biochem. (Tokyo).* 97:1011–1023.

Parry, D. A. D., and J. M. Squire. 1973. Structural role of tropomyosin in muscle regulation: analysis of the X-ray diffraction patterns from relaxed and contracting muscles. *J. Mol. Biol.* 75:33–55.

Perry, S. V. 2003. What is the role of tropomyosin in the regulation of muscle contraction? *J. Muscle Res. Cell Motil.* 24:593–596.

Poole, K. J. V., G. Evans, G. Rosenbaum, M. Lorenz, and K. C. Holmes. 1995. The effect of crossbridges on the calcium sensitivity of the structural change of the regulated thin filament. *Biophys. J.* 68:365 (Abstr.).

Resetar, A. M., J. M. Stephens, and J. M. Chalovich. 2002. Troponin-tropomyosin: an allosteric switch or a steric blocker? *Biophys. J.* 83: 1039–1049.

Smith, D. A., and M. A. Geeves. 2003. Cooperative regulation of myosin-actin interactions by a continuous flexible chain II: actin-tropomyosin-troponin and regulation by calcium. *Biophys. J.* 84:3168–3180.

Smith, D. A., R. Maytum, and M. A. Geeves. 2003. Cooperative regulation of myosin-actin interactions by a continuous flexible chain I: actin-tropomyosin systems. *Biophys. J.* 84:3155–3167.

Sousa, A. D., and C. S. Farah. 2002. Quantitative analysis of tropomyosin linear polymerization equilibrium as a function of ionic strength. *J. Biol. Chem.* 277:2081–2088.

Spudich, J. A., and S. Watt. 1971. The regulation of rabbit skeletal muscle contraction. I. Biochemical studies of the interaction of the tropomyosin-troponin complex with actin and the proteolytic fragments of myosin. *J. Biol. Chem.* 246:4866–4871.

Thierfelder, L., H. Watkins, C. MacRae, R. Lamas, W. McKenna, H.-P. Vosberg, J. G. Seidman, and C. E. Seidman. 1994. Alpha-tropomyosin and cardiac troponin T mutations cause familial hypertrophic cardiomyopathy: a disease of the sarcomere. *Cell.* 77:701–712.

Tobacman, L. S., and C. A. Butters. 2000. A new model of cooperative myosin-thin filament binding. *J. Biol. Chem.* 275:27587–27593.

Trybus, K. M., and E. W. Taylor. 1980. Kinetic studies of the cooperative binding of subfragment 1 to regulated actin. *Proc. Natl. Acad. Sci. USA.* 77:7209–7213.

Vibert, P., R. Craig, and W. Lehman. 1997. Steric-model for activation of muscle thin filaments. *J. Mol. Biol.* 266:8–14.

Wagner, P. D. 1984. Effect of skeletal muscle myosin light chain 2 on the Ca^{2+}-sensitive interaction of myosin and heavy meromyosin with regulated actin. *Biochemistry.* 23:5950–5956.

Weeds, A. G., and R. S. Taylor. 1975. Separation of subfragment-1 isozymes from rabbit skeletal muscle myosin. *Nature.* 257:54–56.

Williams, D. L., Jr., L. E. Greene, and E. Eisenberg. 1988. Cooperative turning on of myosin subfragment 1 adenosine triphosphatase activity by the troponin-tropomyosin-actin complex. *Biochemistry.* 27:6987–6993.

Zot, A. S., and J. D. Potter. 1987. Structural aspects of troponin-tropomyosin regulation of skeletal muscle contraction. *Annu. Rev. Biophys. Biophys. Chem.* 16:535–539.